Inhibition of Poly(ADP-Ribose) Polymerase Modulates Tumor-Related Gene Expression, Including Hypoxia-Inducible Factor-1 Activation, during Skin Carcinogenesis

David Martin-Oliva,[1,2] Rocío Aguilar-Quesada,[1] Francisco O'Valle,[3,4] Jose Antonio Muñoz-Gámez,[1,4] Rubén Martínez-Romero,[1] Raimundo García del Moral,[3,4] José Mariano Ruiz de Almodóvar,[4] Raquel Villuendas,[5] Miguel Angel Piris,[5] and F. Javier Oliver[1]

[1]Institute of Parasitology and Biomedicine, Consejo Superior de Investigaciones Cientificas; [2]Department of Cell Biology, Faculty of Sciences, [3]Department of Pathology, and [4]IBIMER, University of Granada, Granada, Spain; and [5]Centro Nacional de Investigaciones Oncológicas, Madrid, Spain

Abstract

Poly(ADP-ribose) polymerase (PARP)-1, an enzyme that catalyzes the attachment of ADP ribose to target proteins, acts as a component of enhancer/promoter regulatory complexes. In the present study, we show that pharmacologic inhibition of PARP-1 with 3,4-dihydro-5-[4-(1-piperidinyl)butoxyl]-1(2H)-isoquinolinone (DPQ) results in a strong delay in tumor formation and in a dramatic reduction in tumor size and multiplicity during 7,12-dimethylbenz(*a*)anthracene plus 12-*O*-tetradecanoylphorbol-13-acetate–induced skin carcinogenesis. This observation was parallel with a reduction in the skin inflammatory infiltrate in DPQ-treated mice and tumor vasculogenesis. Inhibition of PARP also affected activator protein-1 (AP-1) activation but not nuclear factor-κB (NF-κB). Using cDNA expression array analysis, a substantial difference in key tumor-related gene expression was found between chemically induced mice treated or not with PARP inhibitor and also between wild-type and *parp-1* knockout mice. Most important differences were found in gene expression for *Nfkbiz, S100a9, Hif-1α*, and other genes involved in carcinogenesis and inflammation. These results were corroborated by real-time PCR. Moreover, the transcriptional activity of hypoxia-inducible factor-1α (HIF-1α) was compromised by PARP inhibition or in PARP-1–deficient cells, as measured by gene reporter assays and the expression of key target genes for HIF-1α. Tumor vasculature was also strongly inhibited in PARP-1–deficient mice and by DPQ. In summary, this study shows that inhibition of PARP on itself is able to control tumor growth, and PARP inhibition or genetic deletion of PARP-1 prevents from tumor promotion through their ability to cooperate with the activation AP-1, NF-κB, and HIF-1α. (Cancer Res 2006; 66(11): 5744-56)

Introduction

Because of the causal relationship between inflammation and tumor promotion, different proinflammatory cytokines and enzymes have been implicated in the pathophysiology of human cancer (1), and tumor microenvironment, which is largely orchestrated by inflammatory cells, is an indispensable participant in the neoplastic process, fostering proliferation, survival, and migration. Treatment with potent anti-inflammatory substances is anticipated to exert chemopreventive effect particularly in the promotion stage. Numerous intracellular signaling, including cytokines, mitogens, phorbol esters, growth factors, environmental, and ionizing radiation, converge with the activation of nuclear factor-κB (NF-κB) and activator protein-1 (AP-1), which act independently or coordinately to regulate expression of target genes. These ubiquitous eukaryotic transcription factors mediate pleiotropic effects on cellular transformation and tumor promotion.

A different level of regulation in tumor progression is controlled by the response of tumor to hypoxic condition; hypoxia is a common characteristic of locally advanced solid tumors that have been associated with diminished therapeutic response and malignant progression. The transcription factor hypoxia-inducible factor-1 (HIF-1) is a major regulator of tumor cell adaptation to hypoxic stress (2). Tumor cells with proteomic and genomic changes favoring survival under hypoxic conditions will proliferate, thereby further aggravating the hypoxia. The selection and expansion of new (and more aggressive) clones, which eventually become the dominant tumor cell type, lead to the establishment of a vicious circle of hypoxia and malignant progression.

Poly(ADP-ribose) polymerase (PARP)-1 is the principal member of a family of enzymes possessing poly(ADP-ribosylation) catalytic capacity. It is a conserved nuclear protein that binds rapidly and directly to both single-strand and double-strand breaks. Both processes activate the catalytic capacity of the enzyme, which in turn modulates the activity of a wide range of nuclear proteins by covalent attachment of branching chains of ADP-ribose moieties. Organisms and cellular systems deficient in functional PARP-1 display severely impaired base excision repair and genomic instability, suggesting that the enzyme plays a primary role in the cellular response to DNA damage (3).

Increasing interest in potential clinical applications of PARP inhibition has led to the development of a wide range of new compounds, the more recently developed of which display greatly increased potency and specificity compared with the prototype PARP inhibitor, 3-aminobenzamide (3-AB; ref. 4). The understanding of the role and involvement of PARP-1 in many biological mechanisms, health, and diseases as well as its role in carcinogenesis has steadily increased in recent years. (5). In a previous report, we have shown that *parp-1* knockout (KO) mice are protected against chemically induced skin carcinogenesis (6). In

Note: Supplementary data for this article are available at Cancer Research Online (http://cancerres.aacrjournals.org/).

Requests for reprints: F. Javier Oliver, Instituto de Parasitología y Biomedicina, Consejo Superior de Investigaciones Cientificas, Avda del Conocimiento s/n, 18100 Armilla, Granada, Spain. Phone: 34-958-181655; Fax: 34-958-181632; E-mail: joliver@ipb.csic.es.

doi:10.1158/0008-5472.CAN-05-3050

the present study, we show that the inhibition of PARP activity prevents from tumor growth during skin carcinogenesis due to its ability to modulate the activity of key transcription factors involved in tumor promotion (such as AP-1 and HIF-1) and also to interfere with the expression of genes involved in both tumor promotion/progression and inflammation.

Materials and Methods

Mice/tumor induction experiments and cell culture conditions. Tumor induction in mice on the C57BL/6 background was done as described previously (6), except that one group was treated with 3,4-dihydro-5-[4-(1-piperidinyl)butoxyl]-1(2H)-isoquinolinone (DPQ; Alexis Biochemicals, San Diego, CA), inhibitor of PARP, and applied simultaneously with 12-*O*-tetradecanoylphorbol-13-acetate (TPA). Control animals were also treated in parallel with acetone alone. Visible skin tumors were counted weekly, and the experiment was terminated at week 25. The incidence of papilloma, expressed as the percentage of animals with one or more papillomas, and its papilloma, expressed as the number of papillomas per surviving mouse, were calculated each time tumors were counted.

A short initiation/promotion protocol was used to assess for changes in NF-κB and AP-1 activation, HIF-1α, and genomic expression profiles of skin epithelial cells in the initial steps of carcinogenesis with or without DPQ inhibitor as that by Martin-Oliva et al. (6). This treatment consisted in a single dose of 7,12-dimethylbenz(*a*)anthracene (DMBA; 25 μg) and four doses of 12 μg TPA with or without 30 μg DPQ given 7 days (6) before evaluation of NF-κB and AP-1 activation, HIF-1α, and differential genes expression.

Immortalized mouse embryonic fibroblasts (3T3) from either *parp-1*$^{+/+}$ and *parp-1*$^{-/-}$ mice were cultured at 37°C (5% CO_2) in DMEM containing 10% fetal bovine serum, 0.5% gentamicin (Sigma, St. Louis, MO), and 4.5% glucose.

NF-κB, AP-1, and HIF-1α–binding activity. Gel shift assays were used to detect NF-κB, AP-1, and HIF-1α–binding activity as that by Martin-Oliva et al. (6) and Lok et al. (7).

RNA isolation. DMBA and TPA or TPA plus DPQ were applied to the skin of the backs of mice as described above for gel shift assays. Total RNA was isolated from the skin of the mice 24 hours after the last TPA or TPA plus DPQ treatment by Trizol (Life Technologies, Inc., Gaithersburg, MD) extraction method, then purified with the RNeasy kit (Qiagen, Inc., Valencia, CA), and digested with RNase-free DNase I following the manufacturer's instructions.

Construction and analysis of cDNA microarray. For all microarray studies, the mouse CNIO OncoChip was used. The mouse CNIO OncoChip is a cDNA microarray that has been designed for looking at genes involved in cancer and contains both the NIA15K and the 7.4K clone sets from the National Institute on Aging (http://lgsun.grc.nia.nih.gov/cDNA/cDNA.html) plus additional 600 clones specifically associated to cancer, angiogenesis, apoptosis, signal transduction, and stress processes. Briefly, the mouse cDNA microarray consists of 15,747 unique cDNA clones (rearrayed among 52,374 expressed sequence tags from preimplantation and periimplantation embryos, E12.5 female gonad/mesonephros, and newborn ovary) and 50% novel genes with an average insert size of 1.5 kb (8).

Target preparation. T-7-based RNA amplifications and preparations of cDNA probes were done as described previously (9, 10).

Data analysis. Fluorescence intensity measurements from each array element were compared with local background, and background subtraction was done as that by Tamames et al. (11).

Reverse transcription reaction. Amplified RNA (0.2 μg) was used in 20 μL reverse transcription reaction to synthesize cDNA using the iScript cDNA Synthesis kit (Bio-Rad Laboratories, Hercules, CA) according to the manufacturer's protocol. A detailed description is included in Fig. 3.

Quantitative PCR. Real-time PCR analysis was done using iQ SYBR Green Supermix and the iCycler iQ detection system (Bio-Rad Laboratories) according to the manufacturer's protocol. The sequences of primers used for these studies are shown in Supplementary Table S1. We used the 18S rRNA (12) as endogenous control gene.

Hypoxia mimicking treatment, transient transfection, and Western blot analysis. Hypoxic conditions were mimicked using the iron chelator deferrioxamine (DFO; 200 μmol/L; Sigma), a nonselective prolyl 4-hydroxylase inhibitor. Experimental conditions are explained in Fig. 4. Western blot analysis was done as described previously (13) using an anti-HIF-1α antibody (Bethyl Laboratories, Montgomery, TX).

Histologic techniques. Histologic techniques for conventional morphology and evaluation of blood vessels density were done according to previously published techniques (6).

Statistical analysis. For data shown in Fig. 1*A, i*, we have fitted the values of the average number of tumors per mouse during carcinogenesis treatment using the Mann-Whitney *U* test. Statistical analysis of other experiments used unpaired Student's *t* test.

Results

Inhibition of PARP activity delayed tumor promotion. To test the effect of the inhibition of the catalytic activity of PARP in skin tumor promotion, we treated mice with a single dose of DMBA plus TPA twice weekly with or without the PARP inhibitor DPQ for 25 weeks (see tumor induction experiments in Materials and Methods). Before analyzing the antitumor effect of DPQ, we confirmed in both skin and fibroblasts the inhibitory effect of DPQ in PARP activity, confirming the high potency and low toxicity of this inhibitor at the dose used (results not shown). Papillomas were first found in the TPA mice 8 weeks after promotion, although TPA plus DPQ mice developed tumors starting at week 10, 2 weeks later than carcinogen-treated mice. Tumor multiplicity, found after papilloma promotion, is similar to previously reported data for *parp-1* KO versus wild-type (WT) mice (6). A total of 4.6 papillomas per mouse ($n = 10$) and 1.7 papillomas per mouse ($n = 13$) in TPA and TPA plus DPQ–treated mice, respectively, developed at the end of the treatment (Fig. 1*A, i*). The differences in the number of tumor per mice obtained during the 25 weeks were statistically significant between these two groups of mice ($P < 0.05$). The percentage of tumor-bearing mice at the end of the treatment was 90% for TPA-treated mice ($n = 10$) versus 69.2% for TPA plus DPQ–treated mice ($n = 13$; Fig. 1*A, ii*). DPQ-treated mice, however, started to lose papillomas at week 25. This was due to the fact that these papillomas from DPQ-treated mice presented a fragile, tubular-like morphology (Fig. 1*A, iii*). The papilloma latent period (number of weeks to obtain at least one papilloma per mice) for TPA-treated mice was ~10.4 weeks, whereas TPA plus DPQ–treated mice was 16.6 weeks, suggesting that the time of tumor latency in TPA plus DPQ–treated mice is delayed with respect to the TPA-treated mice. Figure 1*A* (*iii*) shows the difference in the number of tumor per mice and sizes between these two groups of mice taken at the end of carcinogen treatment. In TPA plus DPQ–treated mice, the number and size of papillomas were reduced compared with TPA-treated mice (Table 1). Therefore, this decrease may be attributed to the absence of PARP activity per se.

Histologic examination shows that the epithelium of all mice treated with TPA (without DPQ) developed epithelial hyperplasia with significant increase and irregular thickness of epithelium (0.096 mm; $P < 0.0001$) and granulosum stratum (Fig. 1*B, iii*) versus control (Fig. 1*B, i*) and TPA plus DPQ–treated (Fig. 1*B, ii*) mice. In TPA plus DPQ–treated mice, epithelium is compounded by two or three layers of cells with very thin granulosum stratum, in some cases absent, and scant corneum stratum and a homogeneous thickness of a maximum of 0.02 mm at the end of treatment in the epidermis without lesion (Fig. 1*B, ii*). This homogeneous thickness is similar to control mice treated with acetone alone (0.019 mm; Fig. 1*B, i*).

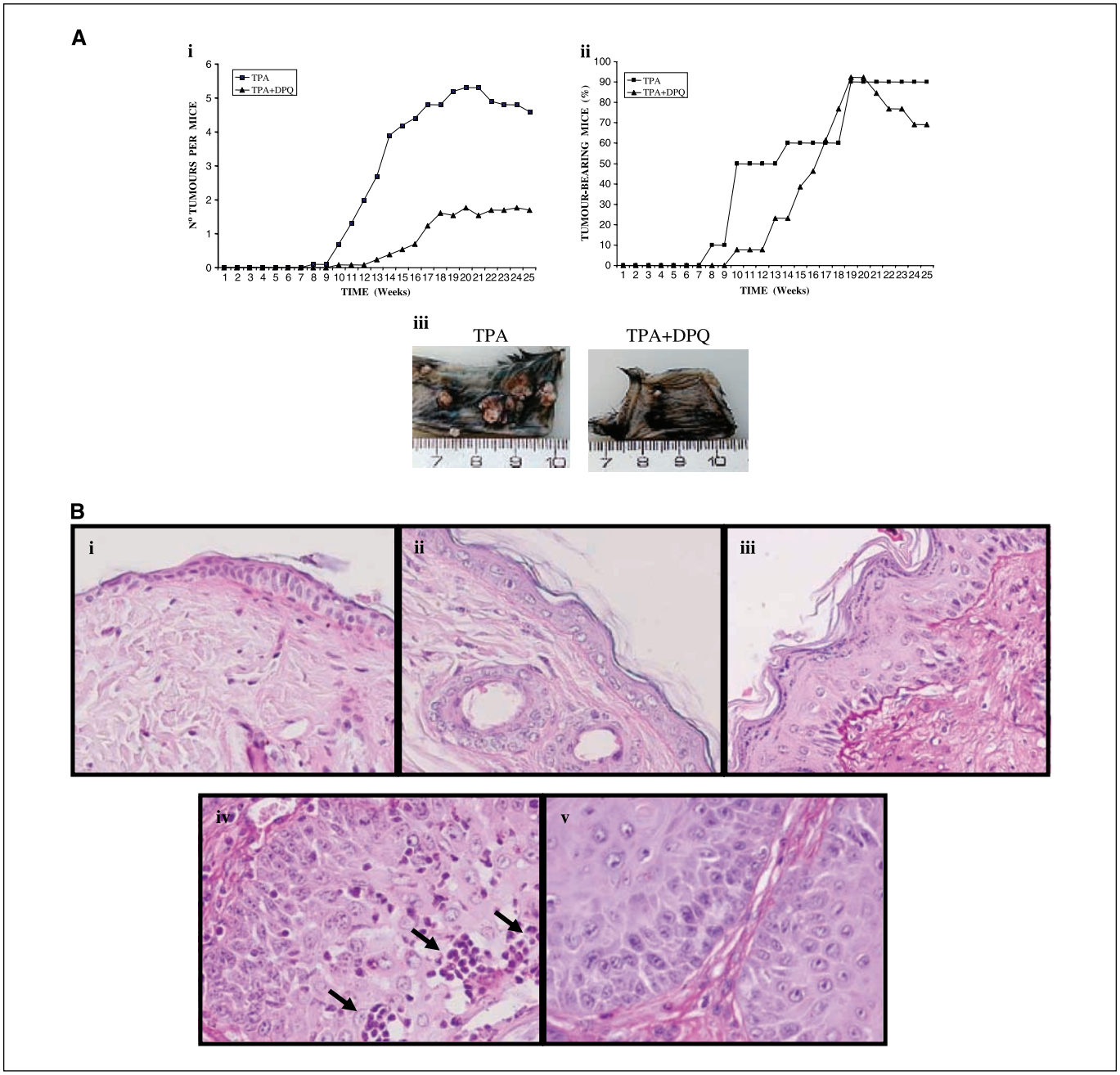

Figure 1. Skin carcinogenesis in mice treated with the PARP inhibitor DPQ. C57BL/6 mice were treated with one dose of 25 μg DMBA and then with 12 μg TPA with or without 30 μg DPQ twice weekly for 25 weeks. Tumors were counted every week. *A, i* to *iii,* tumor multiplicity, incidence, and tumor size at the end of carcinogen treatment. *i,* average number of tumors per mouse by tumor promotion in TPA-treated mice ($n = 10$; ■) and TPA + DPQ–treated mice ($n = 13$; ▲). The differences in tumor multiplicity are significant between these two groups ($P < 0.05$). *ii,* final number of tumor-bearing mice in TPA ($n = 10$; ■) and TPA + DPQ–treated mice ($n = 13$; ▲). *iii,* examples of skin papilloma size in TPA (*left*) and TPA + DPQ–treated mice (*right*) at the end of carcinogen treatment. The tumors were measured with a caliper. *B, i* to *v,* morphologic evaluation of epithelial hyperplasia and skin inflammation. For quantitative evaluation, skin longitudinal tissue sections of TPA-treated mice ($n = 6$), TPA + DPQ–treated mice ($n = 6$), and untreated control mice ($n = 2$) were stained with procedure periodic acid-Schiff (PAS). *i,* homogeneous thickness of epithelium in untreated control. This epithelium is compounded by two or three layers of cells with very thin granulosum stratum and scant corneum stratum (PAS ×400). *ii,* epithelium of TPA + DPQ–treated mice with morphology similar to nontreated control mice (PAS ×400). *iii,* irregular thickness of epithelium and granulosum stratum in mice treated with DMBA + TPA that show epithelial hyperplasia (PAS ×400). *iv* and *v,* mice treated with DMBA + TPA with evident acute and chronic inflammatory infiltrate in papilloma (PAS ×400; *iv*) or treated with TPA + DPQ (*v*), where no signs of inflammatory infiltrate were found. *C, i* to *iii,* histologic examination and diagnosis of inflammation, cell proliferation, and apoptosis in tumors and nonlesional-treated skin. *i,* number of mice with presence of inflammatory infiltrate in the papillomatous lesion. Presence of inflammatory infiltrate in papilloma was assessed by examining their presence in 10 high-power field at ×400 magnification per mouse in treated skin with a single dose of DMBA and promotion with TPA or with TPA + DPQ during 25 weeks. *ii,* number of mastocytes per mm^2 in papilloma from TPA mice and TPA + DPQ–treated mice during 25 weeks. Mastocytes were counted by examining their number in 10 high-power field at ×400 magnification per mouse in nonlesional control (*C*) mice and lesional back skin from treated mice. *iii,* increased cell turnover in skin of TPA-treated mice versus TPA + DPQ–treated and control mice. The average number of mitotic and apoptotic cells was determined by examining their number in 10 high-power field at ×600 magnification per mouse in nonlesional treated mice (*left*) and lesional back skin from treated mice (*right*). *TPA,* skin treated with DMBA plus TPA; *TPA + DPQ,* skin treated with DMBA plus TPA + DPQ. *D,* decreased angiogenesis in DPQ-treated tumors. *Left,* tumor blood vessels were stained with an antibody against lectin as described in Materials and Methods; *right,* quantitation of blood vessels per mm^2 in tumors. *Columns,* mean of at least five different mice in each case; *bars,* SE. *, $P < 0.05$, with respect to control and TPA + DPQ–treated mice; **, $P < 0.01$, with respect to control and TPA + DPQ–treated mice; ***, $P < 0.0001$, with respect to control and TPA + DPQ–treated mice.

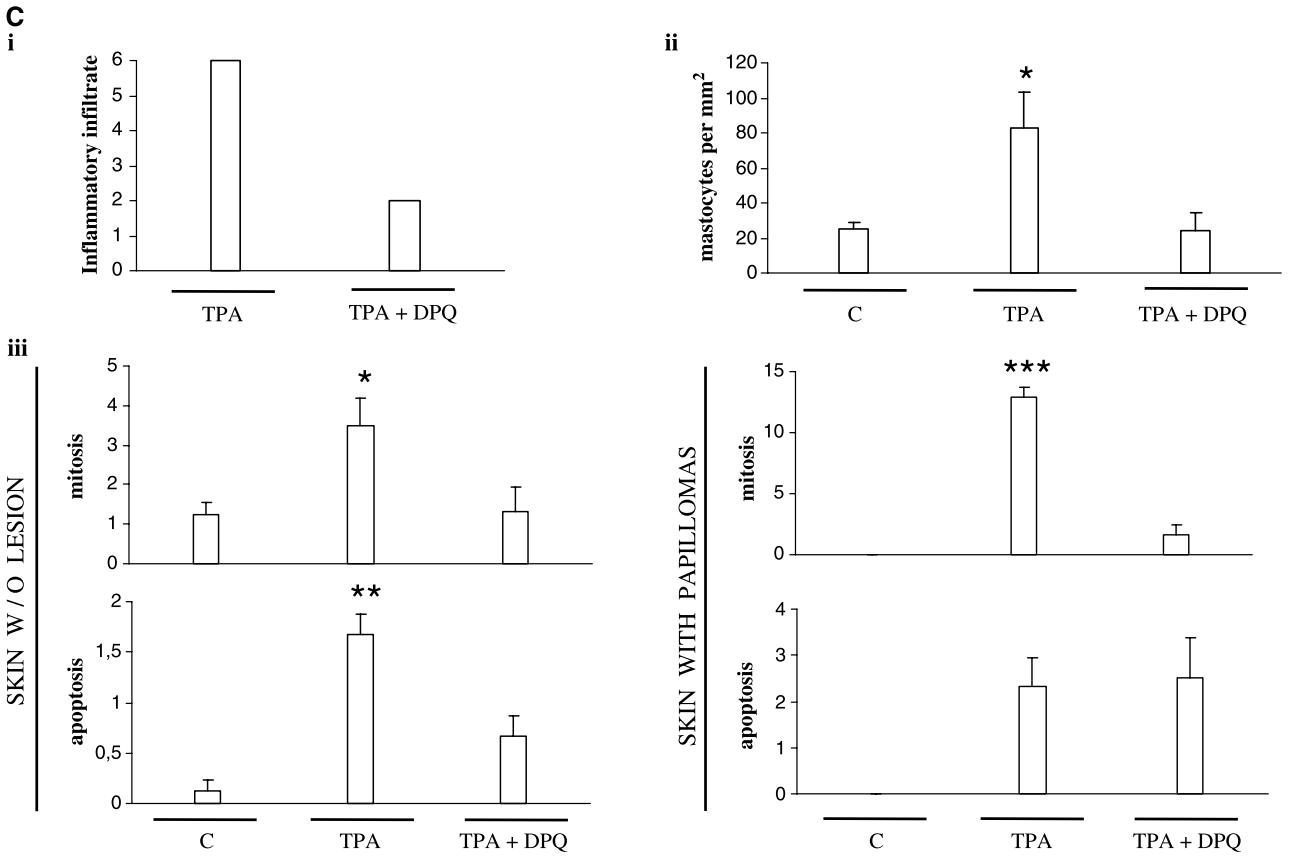

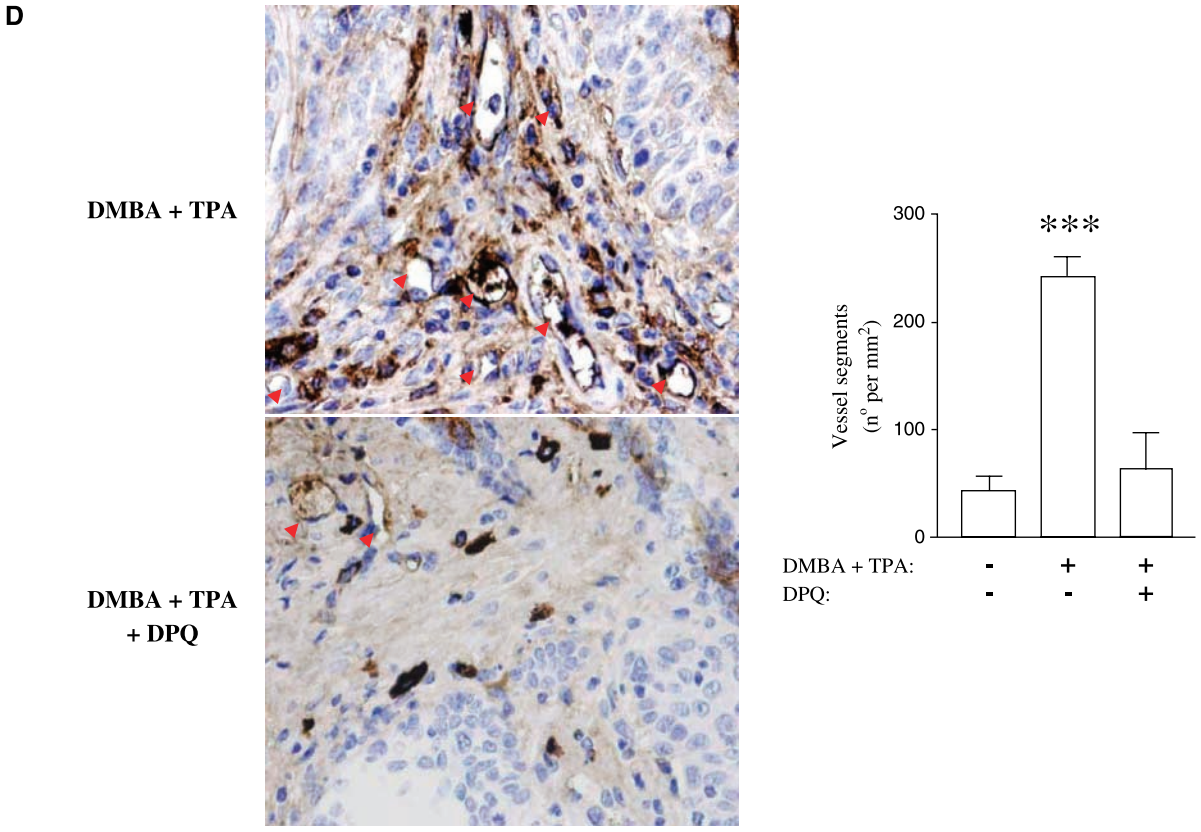

Table 1. Percentage and total numbers of papillomas of different sizes in diameter at the end of carcinogen treatment

Tumors (mm)	Total no. papillomas		% Papillomas	
	TPA (*n*=10)	TPA + DPQ (*n*=13)	TPA	TPA + DPQ
>5	6	2	16.2	8.7
1-5	31	12	83.8	52.2
<1	0	9	0	39.1

The presence of acute inflammatory infiltrate [TPA-treated skin (Fig. 1*B, iv*) and TPA plus DPQ–treated skin (Fig. 1*B, v*); see also Fig. 1*C, i*] and the number of mastocytes per mm^2 in papilloma (Fig. 1*C, ii*) are significantly decreased in TPA plus DPQ–treated mice versus TPA-treated mice ($P < 0.05$). The presence of elevated infiltrates of mastocytes has been correlated with increased vascularization. Cell proliferation is also clearly increased in the papillomas and in the skin without lesion of TPA-treated mice versus TPA plus DPQ–treated mice, displaying an important increased mitosis in tumors (12.2 per high-power field versus 1.7 per high-power field, respectively; $P < 0.0001$; Fig. 1*C, iii*). A striking difference was found in the apoptotic versus mitotic rate between DMBA plus TPA–treated mice and DPQ-treated mice. This accelerated apoptotic activity in DPQ-treated mice may explain why the percentage of mice bearing tumors can increase to ~90% and then decrease to ~70% (Fig. 1*A, ii*).

To analyze tumor-associated vascularization, papillomas of varying sizes were stained with lectin Ulex europaeus biotin conjugated. The "angiogenic switch" from vascular quiescence to up-regulation of angiogenesis was observed in the early stages of skin carcinogenesis (data not shown). Quantitation of vessel density in papilloma showed an important decrease in DPQ-treated mice (Fig. 1*D*), revealing that differences in tumor vascularity may account for the decreased size and incidence after treatment with the PARP inhibitor.

Decrease of AP-1 DNA-binding activity but not NF-κB during tumor promotion after inhibition of PARP. Activation

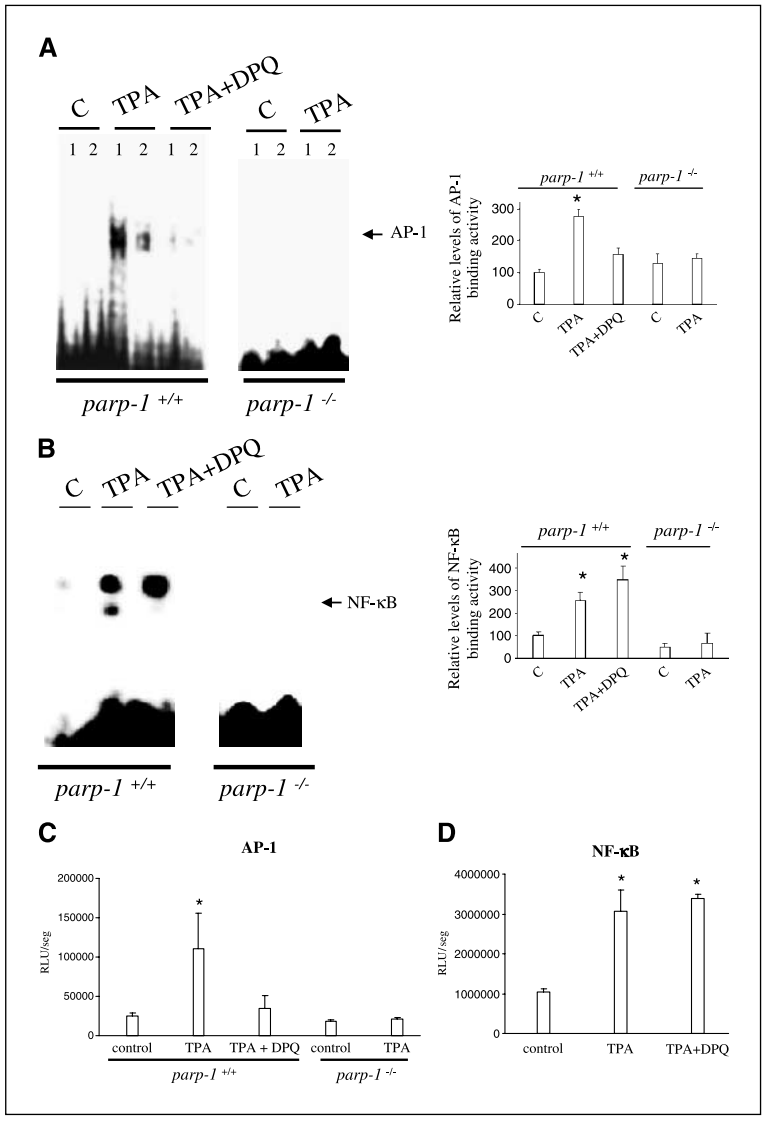

Figure 2. NF-κB and AP-1 DNA-binding activity in TPA or TPA + DPQ–treated mice during tumor promotion. *A,* band shift analysis of AP-1 activation using AP-1-binding promoter sequence in untreated (*C*) and treated skin of *parp-1*$^{+/+}$ and *parp-1*$^{-/-}$ mice with one dose of 25 μg DMBA and four applications of 12 μg TPA together with 30 μg DPQ (TPA + DPQ) or without PARP inhibitor (TPA) as described in Materials and Methods. *1 and 2,* two independent experiments in each condition. *B,* band shift analysis of NF-κB activation using κB iNOS promoter sequence in untreated (*C*) and treated skin of *parp-1*$^{+/+}$ mice with one dose of 25 μg DMBA and four applications of 12 μg TPA together with 30 μg DPQ (TPA + DPQ) or without inhibitor (TPA) as described in Materials and Methods. Representative of four independent experiments. *Right,* quantitation of four independent experiments. *, $P < 0.01$. *C* and *D,* AP-1 and NF-κB luciferase reporter assays. Fibroblasts derived from either *parp-1*$^{+/+}$ or *parp-1*$^{-/-}$ mice were transfected as specified in Materials and Methods and treated with 12 μg TPA or TPA + DPQ (30 μg) in a final volume of 3 mL culture medium for 24 hours. *, $P < 0.05$, with respect to the rest of experimental conditions.

of both AP-1 and NF-κB shows progressive elevation in human and mouse keratinocyte progression models (14). Thus, the observation that targeting AP-1 and NF-κB elevation prevents tumor promotion and progression has been extended from the mouse JB6 model to mouse and human keratinocyte progression models (15). *Parp-1* KO fibroblasts and mice deficient in PARP-1 display a decreased activation of the transcription factor NF-κB (16, 17) and AP-1 (18). To find a mechanistic explanation for the reduced and delayed papilloma formation in mice treated with DPQ, we determined activation of these transcription factors. In nuclear extracts from the epidermis of TPA-treated mice, TPA markedly induced AP-1 and NF-κB activation. However, in the skin of TPA plus DPQ–treated mice and TPA-treated *parp-1* KO mice, there was no activation of AP-1 during skin carcinogenesis (Fig. 2*A*). In contrast, there was no difference in NF-κB activation in the skin of mice treated with TPA plus PARP inhibitor DPQ (Fig. 2*B*). Our previous report suggested that *parp-1* KO mice treated with TPA display a decreased activation of the transcription factor NF-κB (6). Figure 2*A* and *B* (*right*) shows a densitometric analysis of AP-1 and NF-κB band shift assays. The effect of pharmacologic inhibition of PARP by DPQ in TPA-treated mice results in a significant reduction of the relative levels of AP-1-binding activity compared with mice treated with TPA only (Fig. 2*A*). On the other hand, DPQ treatment to TPA-treated skins does not reduce NF-κB-binding activity compared with carcinogen-treated mice (Fig. 2*B*). Results in Fig. 2*C* and *D* show that AP-1 and NF-κB activation using luciferase reporter assay in fibroblasts derived from *parp-1*$^{+/+}$ and *parp-1*$^{-/-}$ also show the deficient activation of AP-1 after deletion/inhibition of PARP-1, whereas NF-κB is not affected by the use of PARP inhibitors as has been shown by different groups (19).

Analysis of differential gene expression. We used cDNA microarrays to obtain gene expression patterns of treated skins during the first week of tumor promotion. For this purpose, we compared the expression data derived from the skin of mice treated as follows: untreated *parp-1*$^{+/+}$ versus *parp-1*$^{+/+}$ treated with carcinogens (DMBA plus TPA) with or without DPQ; untreated *parp-1*$^{-/-}$ versus *parp-1*$^{-/-}$ treated with carcinogens (DMBA plus TPA).

In this way, we were able to monitor mRNA expression of 4,615 known unique murine genes and 11,096 of unknown or hypothetical proteins. Our means of identifying differentially expressed genes were based on consistent fold change and statistical significance assessed by *t* distribution applied to the average and SE to calculate probability values in each tumor/control skin pair. By using the massive screening method, our objective was to select key cancer-related genes that were differentially expressed in mice treated with the PARP inhibitor.

The genes found differentially expressed in skin treated with carcinogens versus in normal skins belong to a variety of different categories. The up-regulated (Table 2) and the down-regulated genes (Table 2) include genes encoding for signal molecules, tumor-associated genes, molecules involved in cell adhesion, inflammatory, and immune reaction, *red-ox* regulation, different metabolic pathways, etc. Analysis of the mRNAs, which are deregulated (up-regulated or down-regulated) at least 2-fold in TPA plus DPQ–treated skin compared with TPA-treated mice, revealed the following results: 40 genes up-regulated and 29 genes down-regulated in the skin of carcinogen-treated mice; 19 genes up-regulated and 21 genes down-regulated in DPQ-treated mice; and 11 genes up-regulated and 20 genes down-regulated in *parp-1* KO mice treated with carcinogens. These results are summarized in Fig. 3*A*. Cluster analysis of all tumor samples revealed 91 genes that match the arbitrary criterion of 2-fold change in either direction with a statistical significance of $P < 0.01$ (Table 2). Of considerable interest is that, depending on the presence of the PARP inhibitor or in *parp-1* KO mice, each promoted skin sample revealed a somewhat unique expression pattern together with an impressive reduction in both the number of altered genes as well as in the up-regulation of significant genes involved in different cellular functions (Table 2).

Real-time PCR gene expression and HIF-1α protein expression. We confirmed by real-time PCR the up-regulation of some of the known genes involved in inflammation and angiogenesis (*S100a9, Hif-1α*, and *Nfkbiz*; Fig. 3*B, left*) as well as other crucial genes known to have a role in transformation of preneoplastic cells that were not reproducibly up-regulated in the microarray. We have analyzed the expression of *osteopontin* (*OPN*), *cathepsin B* (*CtsB*), *cathepsin L* (*CtsL*), *Pecam-1*, and *Igfbp3* by RT-PCR (Fig. 3*C*). The results show that expression of these genes was greatly influenced by either inhibition or genetic deletion of PARP-1 during carcinogenesis. HIF-1 transcriptional activity is dependent on increased levels of HIF-1α protein and on its heterodimerization with HIF-1β (20). To investigate whether carcinogenesis treatment influences HIF-1 activity by altering expression of HIF-1α, the levels of HIF-1α protein were determined in *parp-1*$^{+/+}$ and *parp-1*$^{-/-}$ mice exposed to the inhibitor DPQ as described in Materials and Methods. HIF-1α expression was clearly absent in DPQ-treated and *parp-1*$^{-/-}$ mice (Fig. 3*B, right*).

The RT-PCR results confirmed the array prediction (Fig. 3*B, left*), but more obvious differences were found in the expression levels of the previously described genes (Table 2). Rest of the selected genes matched the prediction of the array, and the enormous increase in the expression of *S100a9* (calgranulin B), whose overexpression has been related with progression of skin carcinogenesis, is particularly striking (21). Induction of the expression of this chemokine has been also related with the migration of neutrophils to inflammatory sites (22) that constitute a remarkable pathologic event during the process of skin carcinogenesis (Fig. 1*B*).

Regulation of HIF-1α activation by PARP-1. In view of the pivotal role of HIF-1α in carcinogenesis, we have focused particular attention to the regulation of HIF-1α by PARP inhibitors and in PARP-1-deficient cells. Cells were treated with de Fe-chelator DFO (which is an iron chelator and activator of this transcription factor) for the time indicated in Fig. 4 and in Materials and Methods. Reporter gene assays were done using a reporter plasmid containing the luciferase gene under the control of nine hypoxia-responsive elements (HRE; ref. 23). HIF-1 activation was clearly attenuated by DPQ and completely absent in *parp-1*$^{-/-}$ cells (Fig. 4*A, left*). Importantly, treatment of PARP-1-deficient cells with DPQ did not have further effect on the transcriptional activation of HIF-1, suggesting that DPQ was inhibiting specifically PARP-1 but not other PARPs. We confirmed this finding by electrophoretic mobility shift assay (EMSA) in nuclear extracts from PARP-1 WT and PARP-1-deficient cells. We determinated that DFO induced HIF-1 activation in *parp-1*$^{+/+}$ cells. Interestingly, WT cells, treated with DFO plus DPQ, and PARP-1-deficient cells showed no activation of HIF-1 during hypoxic treatment, as in Fig. 4*A* (*right*).

Protein levels for HIF-1α were also determined (Fig. 4*B*) after activation with DFO. Again, after PARP inactivation and in *parp-1*$^{-/-}$ cells, a down-regulation of HIF-1α protein expression was observed. The expression of HIF-1α target genes was determined by real-time

Table 2. Gene names in skin of DPQ untreated WT mice (WT TPA), DPQ-treated WT mice (WT TPA + DPQ), and PARP-1 KO mice (KO TPA) versus control mice during tumor promotion in two independent experiments using microarray analysis

Symbol	2-Fold deregulated gene names	Mean			Gene Ontology Biological Process (http://www.ebi.ac.uk/GOA/)
		WT TPA	WT TPA + DPQ	KO TPA	
(A) 2-Fold up-regulated genes*					
Alb1	*Albumin 1*	2			Transport
Cntn4	*Contactin 4*	2			Cell adhesion, transport
Axl	*AXL receptor tyrosine kinase*	2.46	2.14		Cell growth, protein amino acid phosphorylation, regulation of cell cycle
Bmp15	*Bone morphogenetic protein 15*	3.48	3.03	2.3	Cell growth
Ckmt1	*Creatine kinase mitochondrial 1*	2.83	2.3		Unknown
Ctla2b	*Cytotoxic T lymphocyte-associated protein 2β*	3.25			Unknown
Dbnl	*Drebrin-like*	2.14			Rac protein signal transduction, endocytosis, immune response
Degs	*Degenerative spermatocyte homolog*	2.64			Unknown
Eno1	*Enolase 1, α nonneuron*	2.14	2.14		Glucolisis
Expi	*Extracellular proteinase inhibitor*	3.25			Unknown
Ly6g6c	*Lymphocyte antigen 6 complex, locus G6C*		2.14		Unknown
Glrx1	*Glutaredoxin 1 (thioltransferase)*	7.46	5.28	3.25	Electron transport
Gltp	*Glycolipid transfer protein*	2.14			Lipid transport, transport
Gm2a	*GM2 ganglioside activator protein*	2.3			Sphingolipid metabolism
Gp49a	*Glycoprotein 49 A*	3.25		2.14	Unknown
Gpx1	*Glutathione peroxidase*	3.48			Induction of apoptosis by oxidative stress, response to oxidative stress, response to ROS
Gpx2	*Glutathione peroxidase 2*		6.96	5.28	Response to reactive oxygen species
Gsta4	*Glutathione S-transferase α4*	3.25			Unknown
Gsto1	*Glutathione S-transferase ω1*	2.64			Metabolism
Hdc	*Histidine decarboxylase*	3.25	2.64		Unknown
Hif-1a †	*Hypoxia inducible factor 1α sub unit*	2.46			Transduction
Hsd3b4	*Hydroxysteroid dehydrogenase-4, δ5-3-β*	2.14			Steroid biosynthesis, C21-steroid hormone biosynthesis
Ier3	*Immediate early response 3*	2.64		2.46	Unknown
Il18	*Interleukin-18*	3.73		3.03	Immune response
Itgb4bp	*Integrin β_4 binding protein*		2.14		Integrin-mediated signaling pathway, protein biosynthesis, translational initiation
Klf5	*Kruppel-like factor 5*	2.64			Regulation of transcription
Krt1-18	*Keratin complex 1, acidic, gene 18*		2.14		Cytoskeleton organization and biogenesis
Krt2-8	*Keratin complex 2, basic, gene 18*		2.46		C biogenesis, protein amino acid phosphorylation, response to pathogen...
Lcn2	*Lipocalin 2*	2.83	3.48	4.29	Transport
Lgals7	*Lectin, galactose binding, soluble 7*	4.29	2.46	2.3	Apoptosis
Ly6e	*Lymphocyte antigen 6 complex, locus E*	2.3			Defense response
Lyzs	*Lysozyme*	3.03			Carbohydrate metabolism, cell wall catabolism, cytolysis, defense response
Nfkbiz †	*Nuclear factor of κ light polypeptide gene enhancer in B-cells inhibitor, ζ*	3.03			Immune response, regulation of transcription
Map17	*Membrane-associated protein 17*	3.48	2.14	2.46	Unknown
Mglap	*Matrix γ-carboxyglutamate (gla) protein*		2.3		Regulation of bone mineralization
Npc1	*Niemann Pick type C1*	2.3			Cholesterol transport
Pold2	*Polymerase (DNA directed), δ2, regulatory subunit*	2.3			DNA replication
Ppgb	*Protective protein for β-galactosidase*	2.14			Proteolysis and peptidolysis
S100a9 †	*S100 calcium binding protein A9 (calgranulin B)*	36.76	13	10.56	Unknown
Sgk	*Serum/glucocorticoid-regulated kinase*	2.64	2.83		Apoptosis, protein amino acid phosphorylation

(*Continued on the following page*)

Table 2. Gene names in skin of DPQ untreated WT mice (WT TPA), DPQ-treated WT mice (WT TPA + DPQ), and PARP-1 KO mice (KO TPA) versus control mice during tumor promotion in two independent experiments using microarray analysis (Cont'd)

Symbol	2-Fold deregulated gene names	Mean			Gene Ontology Biological Process (http://www.ebi.ac.uk/GOA/)
		WT TPA	WT TPA + DPQ	KO TPA	
Slc34a2	*Solute carrier family 34 (sodium phosphate), member 2*	2.64			Phosphate transport, transport
Soat1	*Sterol O-acyltransferase 1*	2.14			Cholesterol transport
Tagln2	*Transgelin 2*		2.3		Muscle development
Tnc	*Tenascin C*	3.73		2.46	Unknown
Tfrc	*Transferrin receptor*	2.46			Endocytosis, iron ion homeostasis, proteolysis, and peptidolysis
Trps1	*Trichorhinophalangeal syndrome I (human)*	2			Regulation of transcription
Ucp2	*Uncoupling protein 2, mitochondrial*		2.64		Mitochondrial transport, transport
Ugcg	*UDP-glucose ceramide glucosyltransferase*	2.46			Epidermis development, glucosylceramide and glycosphingolipid biosynthesis
(B) 2-Fold down-regulated genes [‡]					
Anapc7	*Anaphase promoting complex subunit 7*			−2.64	Cell cycle, mitosis, cytokinesis, ubiquitin cycle
Arl6ip	*ADP-ribosylation factor-like 6 interacting protein 1*	−2.14			Cotranslational membrane targeting
Bcl2l	*Bcl2-like 1*	−2.3			Regulation negative of apoptosis, regulation of apoptosis, response to radiation
Calmbp1	*Calmodulin binding protein*		−2.3		Mitosis
Calm2	*Calmodulin 2*	−2			G-protein coupled receptor protein signaling pathway, cell cycle
Catns	*Catenin src*		−3.03		Cell adhesion
Cla3	*Cerebellar ataxia 3*	−2.46	−2.14		Unknown
Col1a1	*Procollagen, type I, α1*		−2.83	−3.03	Cell adhesion, phosphate transport
Col1a2	*Procollagen, type I, α2*		−3.73	−2.83	Cell adhesion, phosphate transport
Col3a1	*Procollagen, type III, α1*		−2.83	−2.3	Cell adhesion, phosphate transport
Epb4.1l4b	*Erythrocyte protein band 4.1-like 4b*	−2.3			Transport
Fasn	*Fatty acid synthase*			−2.3	Biosynthesis, fatty acid biosynthesis
Fgfr2	*Fibroblast growth factor receptor 2*	−2.46			Protein amino acid phosphorylation, regulation of cell proliferation, signal transduction
Gclc	*Glutamate-cysteine ligase, catalytic subunit*	−2.46			glutathione biosynthesis
Hbb-b1	*Hemoglobin, β adult major chain*	−2.64			Hemopoiesis, transport, oxygen transport
Hbb-y	*Hemoglobin Y, β-like embryonic c*	−2.14			Transport, oxygen transport
Hmgb1	*High mobility group box 1*	−2.46			DNA packaging, nitric oxide biosynthesis, transport
Hmgb2	*High mobility group box 2*	−2.3	−2.3		DNA packaging, regulation of transcription
Idb3	*Inhibitor of DNA binding 3*	−2.46	−2.46		Negative regulation of transcription from Pol II promoter
Igfbp5	*Insulin-like growth factor binding protein 5*		−2.14	−2.46	Regulation of cell growth, cell growth and/or maintenance
Itm2a	*Integral membrane protein 2A*			−2.83	Unknown
Stmn1	*Stathmin 1*	−4	−3.25		Intracellular signaling cascade, microtubule depolymerization, mitotic spindle assembly
Mt2	*Metallothionein 2*	−2.3	−2.3	−3.25	Nitric oxide mediated signal transduction, zinc ion homeostasis
Myef2	*Myelin basic protein expression factor 2, repressor*	−2.64			Unknown
Mylpf	*Myosin light chain, phosphorylatable, fast skeletal muscle*			−2.46	Cytoskeleton organization and biogenesis, muscle development

(*Continued on the following page*)

Table 2. Gene names in skin of DPQ untreated WT mice (WT TPA), DPQ-treated WT mice (WT TPA + DPQ), and PARP-1 KO mice (KO TPA) versus control mice during tumor promotion in two independent experiments using microarray analysis (Cont'd)

Symbol	2-Fold deregulated gene names	Mean			Gene Ontology Biological Process (http://www.ebi.ac.uk/GOA/)
		WT TPA	WT TPA + DPQ	KO TPA	
Nap1l1	*Nucleosome assembly protein 1-like 1*	−2.46	−2.14		Nucleosome assembly
Psmb5	*Proteasome (prosome, macropain) subunit, β type 5*			−2.46	Ubiquitin-dependent protein catabolism
Purb	*Purine-rich element binding protein B*	−2.14	−3.25	−3.25	Unknown
Pvrl3	*Poliovirus receptor-related 3*	−3.48	−3.25	−3.73	Cell adhesion, cell-cell adhesion
Slc4a2	*Solute carrier family 4 (anion exchanger), member 2*	−3.03			Ion transport, anion transport, transport
Smarca5	*SWI/SNF-related, matrix-associated, actin-dependent regulator of chromatin*	−2.14	−2.14		Chromatin assembly or disassembly, chromatin remodeling
Sox4	*SRY-box containing gene 4*	−2.83			Regulation of transcription
Spr	*Sepiapterin reductase*	−2.83	−2.46	−3.03	Metabolism, tetrahydrobiopterin biosynthesis
Sp1	*Trans-acting transcription factor 1*		−2.14	−2.3	Regulation of transcription, positive regulation of transcription
Tera	*Teratocarcinoma expressed, serine rich*	−2.64	−2.64	−2	Unknown
Tia1	*Cytotoxic granule-associated RNA-binding protein 1*	−2.46			Apoptosis
Tm4sf6	*Transmembrane 4 superfamily member 6*	−2.83			Unknown
Tnfrsf19	*Tumor necrosis factor receptor superfamily member 19*	−2.46	−2.83	−2.83	Unknown
Ttc3	*Tetratricopeptide repeat domain 3*	−2.14	−2.14	−2.14	Unknown
Tubb5	*Tubulin, β5*	−2.14			Microtubule-based process
Ube2s	*Ubiquitin-conjugating enzyme E2S*			−2.64	Protein modification, ubiquitin cycle
Utrn	*Utrophin*			−2.46	Signal transduction, muscle development, muscle contraction, chemotaxis
5830426I05Rik	*RIKEN cDNA 5830426I05 gene*	−2.14	−2.46	−2.3	Inner cell mass cell proliferation

*Mean gene names with fold <2 between control and treated mice are not indicated.
†Real-time PCR analysis gene expression.
‡Mean gene names with fold greater than −2 between control and treated mice are not indicated.

RT-PCR. The expression of *Igfbp3, Bnip3*, and *Vegf-A* genes was all strongly up-regulated by this drug in WT fibroblasts (Fig. 4*C* and *D*). However, after inhibition of PARP and in cells deficient in PARP-1, there was a deficient activation in the expression of these genes (Fig. 4*C* and *D*).

Discussion

Tumorigenesis is a complex multistage process, in which a series of genetic changes is thought to deregulate the cellular processes that control cell proliferation, differentiation, genome integrity, DNA repair, and induction of apoptosis. The murine model of chemically induced skin carcinogenesis is one of the best defined experimental *in vivo* models of epithelial carcinogenesis, representing an important tool for the understanding of current concepts about human neoplasia, including the multistage nature of tumor development. In this model, the development of squamous cell malignancy of the skin can be subdivided into three phases: initiation, promotion, and progression (24). Although genetic events are crucial to initiation and progression, the rate-limiting step in this model, the tumor promotion, is predominantly characterized by epigenetic events. In this context, changes in the RNA expression level, which are closely related to the amount of protein product and thus the biochemical activity, may be considered as first evidence for a gene with oncogenic potential.

PARP-1 may influence the stress/inflammation response through regulation of transcription factors and associated gene transcription. PARP-1 has been reported to either activate or repress transcription activity (25). PARP-1 influences on transcription activity may involve direct protein-protein interaction with PARP-1 or the catalytic activity of the PARP-1 enzyme, which can poly(ADP-ribosyl)ate transcription factors. Transcription factors, such as AP-2 (26), B-MYB (27), Oct-1 (28), YY-1 (29), and TEF-1 (30), have been shown to bind directly to PARP-1. On the other hand, transcription factors, such as p53 (31), fos (32), and RNA polymerases I and II (25), are poly(ADP-ribosyl)ated. NF-κB transcription activation after stress/inflammatory stimuli is reduced in *parp-1*$^{-/-}$ cells (16, 19).

The global analysis of gene expression during carcinogenesis as function of either PARP inhibition or in the skin of PARP-1-null mice revealed striking differences between the three groups analyzed (Fig. 3*A*; Table 2). Genes up-regulated in carcinogen-treated skin from WT mice (without DPQ treatment) include several tumor-associated genes in mouse and human [i.e., *AXL receptor tyrosine kinase* (*Axl*), *Enolase 1* (*Eno1*), *Hif-1α, immediate*

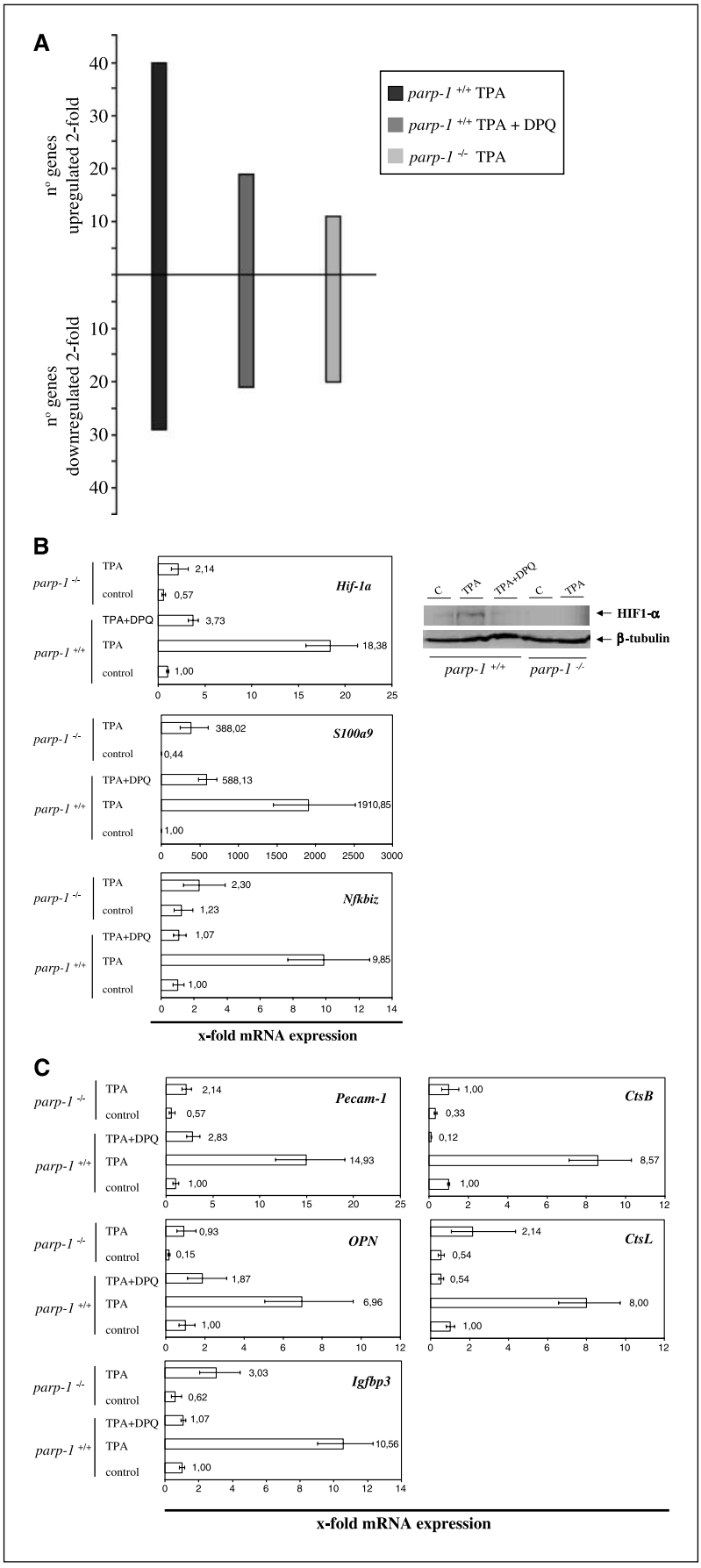

Figure 3. Numbers of genes that are deregulated (up-regulated or down-regulated) by at least 2-fold in carcinogen-treated skin versus normal skin by using cDNA microarray analysis. Twenty-four hours after the short initiation/promotion protocol, RNA was obtained from control, TPA, or TPA + DPQ–treated mice, and amplified RNA was used for hybridization of microarray slide as described in Materials and Methods. For data analysis, fluorescence intensity measurements from each array element were compared with local background, and background subtraction was done. To normalize the data, the Cy3/Cy5 ratio was adjusted using the diagnosis and normalization array data tool. In addition, spots with background-subtracted signal intensities <500 fluorescence units (sum of the two channels) were excluded from the analysis. Furthermore, bad spots or areas of the array with obvious defects were manually flagged. The Cy3/Cy5 ratios of the duplicated spots of the array were averaged. Genes were deemed to be up-regulated or down-regulated if the difference ratio was at least 2-fold. *A,* global gene expression differences between the three groups of mice used in the study: *parp-1*$^{+/+}$ TPA, *parp-1*$^{+/+}$ TPA + DPQ, and *parp-1*$^{-/-}$ TPA. *B* and *C,* differential gene expression measured by quantitative real-time PCR. DMBA and TPA or TPA + DPQ were applied to the skin of the backs of *parp-1*$^{+/+}$ and *parp-1*$^{-/-}$ mice with the short protocol as described in Materials and Methods. Total RNA was isolated from the skin of the mice 24 hours after the last TPA or TPA + DPQ treatment, and 0.2 μg RNA was used in 20 μL RT reaction to synthesize cDNA. *B,* real-time PCR of genes recently identified as possibly NF-κB regulated (*Nfkbiz* or *Mail*), AP-1 regulated (*S100a9* or *calgranulin B*), and *Hif-1α. Right,* expression of HIF-1α protein. *C,* real-time PCR of some of the known genes involved in inflammation and tumor progression: *Pecam-1, OPN, CtsB, CtsL*, and *Igfbp3*. The results were normalized to the expression of 18S rRNA for all of the samples. Real-time PCR analysis was done using iQ SYBR Green Supermix and the iCycler iQ detection system according to the manufacturer's protocol. The sequences of primers used for these studies are shown in Supplementary Table S1. In all cases, a standard curve containing at least four concentrations (represented in triplicate) of a control cDNA was constructed for both the endogenous control gene (18S rRNA) and the gene of interest. In all cases, standard curves had a coefficient of correlation >0.98. For data analysis, the cycle threshold value (C_T; arbitrary number of PCR cycles, in which all of the PCR amplification graphs is comparing, is in the linear range) was calculated in each case. A lower C_T value means more transcript, and a higher C_T value means less transcript. To normalize the endogenous control gene, the gene of interest C_T value was divided by the endogenous control gene C_T value. We used the 18S rRNA endogenous control gene because its level of expression is very stabile and so high that small fluctuations will not result in detectable fluctuations in the normalized fluorescence signal of the target gene. In each case, all samples were represented in triplicate for relative quantitative fold calculations with respect to untreated sample mice.

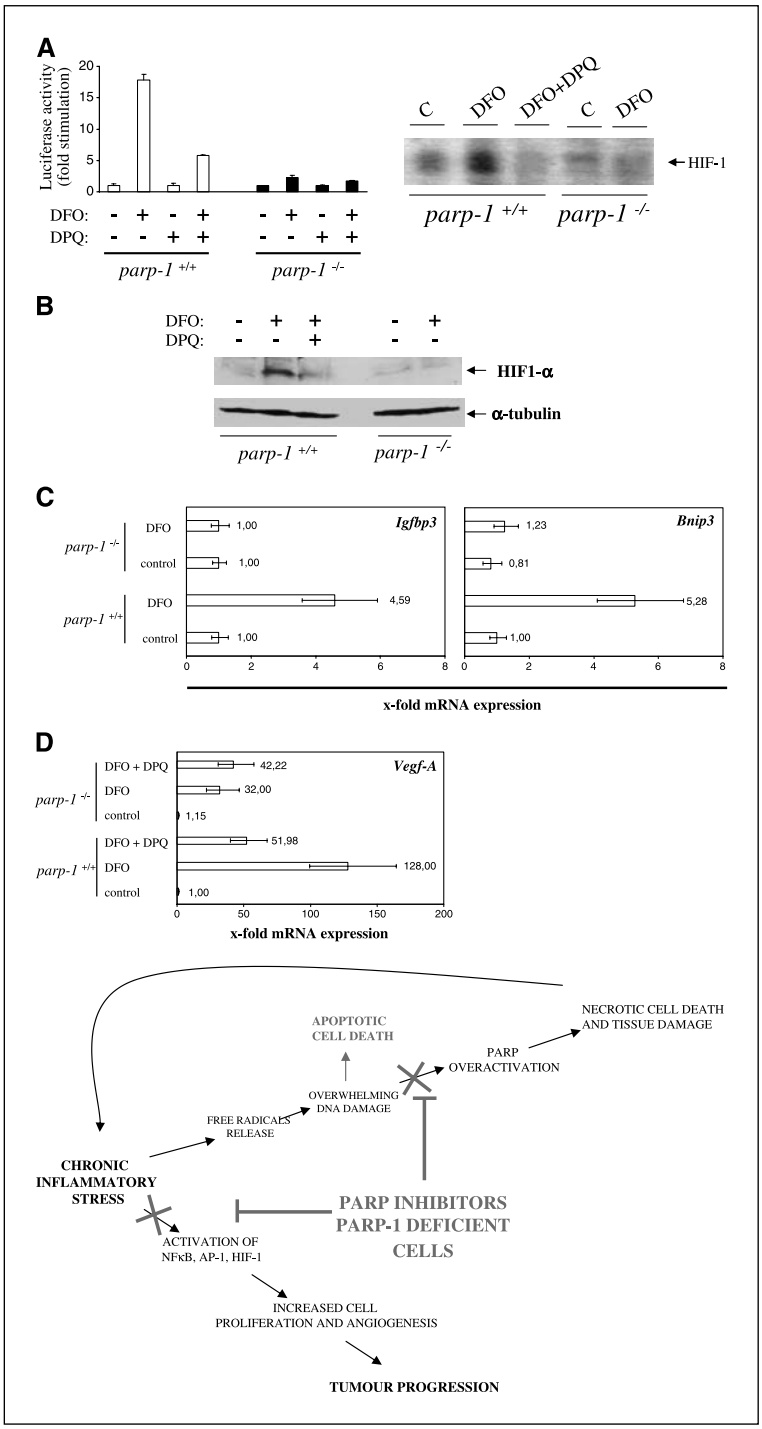

Figure 4. Defective HIF-1–dependent transcriptional activation in DPQ-treated and *parp-1*$^{-/-}$ cells. Cells were transiently cotransfected with 0.25 μg β-galactosidase reporter vector (as control of transfection) together with 1 μg of the HIF/luciferase plasmid (kind gift from Dr. Del Peso, Hospital Universitario de La Princesa, Madrid, Spain) or 1 μg of the NF-κB/luciferase plasmid or 1 μg of the AP-1/luciferase plasmid (both are kind gifts from Dr. López-Rivas, Centro Andaluz de Biologia del Desarrollo-CSIC, Sevilla, Spain) using jetPEI cationic polymer transfection reagent (Polytransfection, Illkirch, France) according to the manufacturer's instructions. *A,* 3T3 *parp-1*$^{+/+}$ and *parp-1*$^{-/-}$ were transfected with a reporter luciferase plasmid containing 9× HRE as described in Materials and Methods. Luciferase activity was measured 36 hours after DFO treatment. EMSA for HIF-1 activation. Conditions for EMSA are explained in Materials and Methods. *B,* protein levels of HIF-1α 24 hours after DFO treatment in 3T3 *parp-1*$^{+/+}$ [with or without DPQ (20 μmol/L)] and *parp-1*$^{-/-}$ cells treated with 200 μmol/L DFO. *C* to *D,* real-time RT-PCR of HIF-1-dependent genes (*Igfbp3, Bnip3*, and *Vegf-A*). mRNA levels were determined 36 hours after DFO treatment. *Columns,* mean of at least three independent experiments done in duplicate and HIF-1α protein levels are representative experiments of three. *D, bottom,* proposed model of action of PARP inhibitor in tumors, in which the inflammatory component is key for their development.

early response 3 (*Ier3; Iex-1*), *Kruppel-like factor 5* (*Klf5*), *calgranulin B* (*S100a9*), *tenascin C* (*Tnc*), *UDP-glucose ceramide glucosyltransferase* (*Ugcg*), *lectin galactose binding soluble 7* (*Lgals7*), *tranferrin receptor* (*Tfrf*), *membrane-associated protein 17* (*Map17*), *lysozyme* (*Lyzs*), *extracellular proteinase inhibitor* (*Expi*), *trichorhinophalangeal syndrome I* (*Trps1*), *Niemann Pick type C1* (*Npc1*), and *serum/glucocorticoid-regulated kinase* (*Sgk*)]; genes involved in oxidative stress, inflammation, and immune response include *glutathione peroxidase 1* (*Gpx1*), *glutathione* S-*transferase α4* (*Gsta4*) and *glutathione* S-*transferase ω1* (*Gsto1*), *interleukin-18* (*Il18*), *Nfkbiz* (also called *Mail*), *glutaredoxin 1* (*Glrx1*), *sterol* O-*acyltransferase* (*Soat-1*), *CTL-associated protein 2b* (*Ctla2b*), *glycoprotein marker of natural killer cells* (*Gp49a*), *lymphocyte antigen 6 complex* (*Ly6e*), and *drebrin-like* (*Dbnl*). All the above genes were either not up-regulated, or the expression significantly decreased with DPQ treatment or in *parp-1*$^{-/-}$ mice (Table 2). Some of the above genes are targets of NF-κB [*Nfkbiz, Iex-1, Tnc, Lyzs*, and *procollagen type I α2* (*Col1a2*); ref. 33] and AP-1 (*Tnc, procollagen type I, S100* family members, and *Pold2*; ref. 34), supporting our previous results that defective activation

of these two key transcription factors by either PARP inhibition or genetic deletion of PARP-1 results in an effective blockage of gene expression. During the promotion of skin carcinogenesis, the expression of several genes is also down-regulated. Of note are some genes that have been reported to be involved in the progression of different human and mouse tumors, which were only down-regulated or the expression significantly decreased with DPQ treatment or in *parp-1*$^{-/-}$ mice (Table 2): dermatofibrosarcoma and skin neoplasms (procollagens type I and III), *Igfbp5b, metallothionein 2* (*Mt2*), *purine-rich element binding protein B* (*Purb*), *trans*-acting transcription factor-1 (*Sp1*), and *fatty acid synthase* (*Fasn*). Other gene 2-fold down-regulated only in carcinogen-treated mice (without DPQ treatment) was the *fibroblast growth factor 2* (*Fgfr2*), whose loss of expression accompanies malignant progression of both animal and human prostate tumors (35).

One of the more important outcome in the current study is the ability of PARP-1/PAR to modulate the expression of genes involved in angiogenesis, particularly *Hif-1α, Pecam-1*, and probably *OPN*. Of particular interest is the absence of induction of *Hif-1α* after treatment with DPQ and in *parp-1*-deficient mice. This transcription factor has been largely involved in tumor progression by promoting global response to hypoxia, including new vessels formation (36). Hypoxia is an almost universal hallmark of solid tumors. Adaptation to hypoxia is critical for tumor survival and growth and is mediated in large part by transcriptional activation of genes that facilitate short-term adaptive mechanisms (e.g., increased vascular permeability, vasodilation, glucose transport, and switch to anaerobic metabolism) as well as long-term adaptive mechanisms. This coordinated homeostatic response is mediated, in large part, through the activation of the heterodimeric transcription factor HIF-1. Tumor hypoxia and overexpression of HIF-1 have been associated with resistance to certain therapies, increased risk of invasion and metastasis, and poor outcome in certain malignancies. The near universality of hypoxia in human tumors and centrality of the HIF pathway may have therapeutic utility as an antitumor strategy. Inhibition of HIF function in tumors may attenuate and contribute directly to tumor cell death through metabolic derangement. This role seems to be accomplished by the PARP inhibitor DPQ because HIF-1α is unable to accumulate after treatment with DPQ (Fig. 4*B*), and increased rates of apoptotic cells are present in the incipient tumors of DPQ-treated mice. Thus, inhibition of PARP could be of great potential interest in the design of new antiangiogenic therapies. Targeting PARP is not only a way to prevent efficient DNA repair during treatment with classic chemotherapy and radiotherapy as has been classically envisaged but also its effective targeting has more general effects on transcription of key genes involved in tumor progression. Up to date, the molecular link between the HIF-1 and PARP-1 has not been identified. What is clear from our results is that stabilization of HIF-1α differs drastically between *wt* and *parp-1*-deficient cells and also in the presence of the PARP inhibitor DPQ. PARP-1 has been reported repeatedly as a transcriptional cofactor of several transcription factor, including NF-κB and AP-1. As a hypothesis, we are working in the possible involvement of CPB/p300 protein as a link between PARP-1 and HIF-1α. CBP binding to HIF-1α is a key step for HIF-1-dependent transcriptional activation, and PARP-1 is a substrate for CBP (CBP-dependent PARP-1 acetylation is necessary for PARP-1 acting as a cofactor of NF-κB activation).

Different groups have proven the benefits of inhibiting PARP-1 in the potentiation of classic antineoplasic treatments, either radiotherapy or chemotherapy (4, 37, 38). In this study, we show that the PARP inhibitor DPQ on itself has antitumor activity. The effect of DPQ on tumor multiplicity, tumor incidence, and tumor size (Fig. 1*A*) clearly indicates that the sole inhibition of PARP is able to slow down tumor growth.

As we have previously shown, genetic deletion of PARP-1 completely prevented TPA-induced cell proliferation, with a clear effect in tumor latency, incidence, and multiplicity (6). Although it is now clear that proliferation of cells alone does not cause cancer, sustained cell proliferation in an environment rich in inflammatory cells and DNA damage-promoting agents (as free radicals derived reactive oxygen and nitrogen species during the inflammatory response do) potentiates and/or promotes neoplastic risk. Our hypothesis is that inhibition or genetic elimination of PARP-1 interferes with the promotion of tumors of epithelial origin, in which inflammatory processes play a critical role in this step (39). The implications of DNA repair inhibitors for anticancer therapy are well recognized (40), and the role of PARP-1 in DNA damage repair has been extensively characterized. First-generation PARP-1 inhibitors, such as 3-AB, lacked the potency, specificity, and pharmacologic properties required for detailed preclinical evaluation of their ability to increase the sensitivity of tumors to anticancer chemotherapy and radiotherapy. New highly potent PARP inhibitors have shown their specificity and *in vivo* activity to enhance chemotherapy and radiotherapy of human cancer (40). More recently, two different groups provided strong evidences in the sense that monotherapy with PARP inhibitors was effective in eliminating BRCA-1 and BRCA-2 cancer cells and tumors due to the inability of these cells to repair by homologous recombination the stalled replication fork damages induced by PARP inhibitors (41, 42).

It is now evident that inflammation has powerful effect on tumor development. As summarized in the proposed model (Fig. 4*D, bottom*), PARP inhibitors may affect tumor progression by interfering with the activation of key transcription factors involved in cell proliferation, angiogenesis, and inflammation. Early in the neoplastic process, proinflammatory factors and cells are powerful tumor promoters, producing an attractive environment for tumor growth, facilitating sustained DNA damage, and promoting angiogenesis. Thus, effective inhibition of PARP might have a clear benefit in antitumor therapy by facilitating a reduced oxidative status (thus minimizing reactive oxygen and nitrogen species release and the DNA damage) and minimizing the activation of proinflammatory and proangiogenic factors.

Acknowledgments

Received 9/7/2005; revised 2/17/2006; accepted 3/23/2006.

Grant support: Grants SAF 2003-01217, RNIHG c03/02, PI050972, and FIS G03/152 (F.J. Oliver), grant PI021505 (R. García del Moral), and grants CICYT SAF 2001-3533 and SAF 2004-00889 (J.M. Ruiz de Almodóvar). D. Martin-Oliva and J.A. Muñoz-Gámez have fellowships from Instituto de Salud Carlos III. R. Aguilar-Quesada is a recipient of Formación de Profesorado Universitario fellowship from the Spanish Ministerio de Educación y Ciencia. R. Martínez-Romero is a recipient of a fellowship I3P from Consejo Superior de Investigaciones Cientificas (CSIC).

The costs of publication of this article were defrayed in part by the payment of page charges. This article must therefore be hereby marked *advertisement* in accordance with 18 U.S.C. Section 1734 solely to indicate this fact.

We thank Francisco Ferrer Gamarra and Dolores Beriso Herranz from the animal house of Instituto de Parasitología y Biomedicina "López Neyra" (CSIC, Granada, Spain), Paloma the la Cueva from Centro Nacional de Investigaciones Oncológicas (Madrid, Spain) for technical assistance in the hybridization of cDNA arrays, and Dr. Gilbert de Murcia (Centre National de la Recherche Scientifique, Strasbourg, France) for the PARP-1-null mice.

References

1. Aggarwal BB. Nuclear factor-κB: the enemy within. Cancer Cell 2004;6:203–8.
2. Vaupel P. The role of hypoxia-induced factors in tumor progression. Oncologist 2004;9 Suppl 5:10–7.
3. Shall S, de Murcia G. Poly(ADP-ribose) polymerase-1: what have we learned from the deficient mouse model? Mutat Res 2000;460:1–15.
4. Miknyoczki SJ, Jones-Bolin S, Pritchard S, et al. Chemopotentiation of temozolomide, irinotecan, and cisplatin activity by CEP-6800, a poly(ADP-ribose) polymerase inhibitor. Mol Cancer Ther 2003;2:371–82.
5. Masutani M, Nakagama H, Sugimura T. Poly(ADP-ribose) and carcinogenesis. Genes Chromosomes Cancer 2003;38:339–48.
6. Martin-Oliva D, O'Valle F, Munoz-Gamez JA, et al. Crosstalk between PARP-1 and NF-κB modulates the promotion of skin neoplasia. Oncogene 2004;23:5275–83.
7. Lok CN, Ponka P. Identification of a hypoxia response element in the transferrin receptor gene. J Biol Chem 1999;274:24147–52.
8. Fraga MF, Herranz M, Espada J, et al. A mouse skin multistage carcinogenesis model reflects the aberrant DNA methylation patterns of human tumors. Cancer Res 2004;64:5527–34.
9. Van Gelder RN, von Zastrow ME, Yool A, et al. Amplified RNA synthesized from limited quantities of heterogeneous cDNA. Proc Natl Acad Sci U S A 1990;87:1663–7.
10. Eberwine J. Amplification of mRNA populations using aRNA generated from immobilized oligo(dT)-T7 primed cDNA. BioTechniques 1996;20:584–91.
11. Tamames J, Clark D, Herrero J, et al. Bioinformatics methods for the analysis of expression arrays: data clustering and information extraction. J Biotechnol 2002;98:269–83.
12. Burbach GJ, Dehn D, Del Turco D, Deller T. Quantification of layer-specific gene expression in the hippocampus: effective use of laser microdissection in combination with quantitative RT-PCR. J Neurosci Methods 2003;131:83–91.
13. Munoz-Gamez JA, Martin-Oliva D, Aguilar-Quesada R, et al. PARP inhibition sensitizes p53-deficient breast cancer cells to doxorubicin-induced apoptosis. Biochem J 2005;386:119–25.
14. Li JJ, Dong Z, Dawson MI, Colburn NH. Inhibition of tumor promoter-induced transformation by retinoids that transrepress AP-1 without transactivating retinoic acid response element. Cancer Res 1996;56:483–9.
15. Bernstein LR, Colburn NH. AP1/jun function is differentially induced in promotion-sensitive and resistant JB6 cells. Science 1989;244:566–9.
16. Oliver FJ, Menissier-de Murcia J, Nacci C, et al. Resistance to endotoxic shock as a consequence of defective NF-κB activation in poly(ADP-ribose) polymerase-1 deficient mice. EMBO J 1999;18:4446–54.
17. Hassa PO, Buerki C, Lombardi C, Imhof R, Hottiger MO. Transcriptional coactivation of nuclear factor-κB-dependent gene expression by p300 is regulated by poly(ADP)-ribose polymerase-1. J Biol Chem 2003;278:45145–53.
18. Andreone TL, O'Connor M, Denenberg A, Hake PW, Zingarelli B. Poly(ADP-ribose) polymerase-1 regulates activation of activator protein-1 in murine fibroblasts. J Immunol 2003;170:2113–20.
19. Hassa PO, Covic M, Hasan S, Imhof R, Hottiger MO. The enzymatic and DNA binding activity of PARP-1 are not required for NF-κ B coactivator function. J Biol Chem 2001;276:45588–97.
20. Wang GL, Semenza GL. Characterization of hypoxia-inducible factor 1 and regulation of DNA binding activity by hypoxia. J Biol Chem 1993;268:21513–8.
21. Gebhardt C, Breitenbach U, Tuckermann JP, et al. Calgranulins S100A8 and S100A9 are negatively regulated by glucocorticoids in a c-Fos-dependent manner and overexpressed throughout skin carcinogenesis. Oncogene 2002;21:4266–76.
22. Vandal K, Rouleau P, Boivin A, et al. Blockade of S100A8 and S100A9 suppresses neutrophil migration in response to lipopolysaccharide. J Immunol 2003;171:2602–9.
23. Alvarez-Tejado M, Alfranca A, Aragones J, et al. Lack of evidence for the involvement of the phosphoinositide 3-kinase/Akt pathway in the activation of hypoxia-inducible factors by low oxygen tension. J Biol Chem 2002;277:13508–17.
24. Marks F, Furstenberger G. The conversion stage of skin carcinogenesis. Carcinogenesis 1990;11:2085–92.
25. D'Amours D, Desnoyers S, D'Silva I, Poirier GG. Poly(ADP-ribosyl)ation reactions in the regulation of nuclear functions. Biochem J 1999;342:249–68.
26. Kannan P, Yu Y, Wankhade S, Tainsky MA. PolyADP-ribose polymerase is a coactivator for AP-2-mediated transcriptional activation. Nucleic Acids Res 1999;27:866–74.
27. Cervellera MN, Sala A. Poly(ADP-ribose) polymerase is a B-MYB coactivator. J Biol Chem 2000;275:10692–6.
28. Nie J, Sakamoto S, Song D, Qu Z, Ota K, Taniguchi T. Interaction of Oct-1 and automodification domain of poly(ADP-ribose) synthetase. FEBS Lett 1998;424:27–32.
29. Oei SL, Griesenbeck J, Schweiger M, et al. Interaction of the transcription factor YY1 with human poly(ADP-ribosyl) transferase. Biochem Biophys Res Commun 1997;240:108–11.
30. Butler AJ, Ordahl CP. Poly(ADP-ribose) polymerase binds with transcription enhancer factor 1 to MCAT1 elements to regulate muscle-specific transcription. Mol Cell Biol 1999;19:296–306.
31. Wesierska-Gadek J, Schmid G. Poly(ADP-ribose) polymerase-1 regulates the stability of the wild-type p53 protein. Cell Mol Biol Lett 2001;6:117–40.
32. Amstad PA, Krupitza G, Cerutti PA. Mechanism of c-*fos* induction by active oxygen. Cancer Res 1992;52:3952–60.
33. Pahl HL. Activators and target genes of Rel/NF-κB transcription factors. Oncogene 1999;18:6853–66.
34. Schlingemann J, Hess J, Wrobel G, et al. Profile of gene expression induced by the tumour promotor TPA in murine epithelial cells. Int J Cancer 2003;104:699–708.
35. Yasumoto H, Matsubara A, Mutaguchi K, Usui T, McKeehan WL. Restoration of fibroblast growth factor receptor2 suppresses growth and tumorigenicity of malignant human prostate carcinoma PC-3 cells. Prostate 2004;61:236–42.
36. Yeo EJ, Chun YS, Park JW. New anticancer strategies targeting HIF-1. Biochem Pharmacol 2004;68:1061–9.
37. Bowman KJ, White A, Golding BT, Griffin RJ, Curtin NJ. Potentiation of anti-cancer agent cytotoxicity by the potent poly(ADP-ribose) polymerase inhibitors NU1025 and NU1064. Br J Cancer 1998;78:1269–77.
38. Tentori L, Leonetti C, Scarsella M, et al. Combined treatment with temozolomide and poly(ADP-ribose) polymerase inhibitor enhances survival of mice bearing hematologic malignancy at the central nervous system site. Blood 2002;99:2241–4.
39. Coussens LM, Werb Z. Inflammation and cancer. Nature 2002;420:860–7.
40. Calabrese CR, Almassy R, Barton S, et al. Anticancer chemosensitization and radiosensitization by the novel poly(ADP-ribose) polymerase-1 inhibitor AG14361. J Natl Cancer Inst 2004;96:56–67.
41. Farmer H, McCabe N, Lord CJ, et al. Targeting the DNA repair defect in BRCA mutant cells as a therapeutic strategy. Nature 2005;434:917–21.
42. Bryant HE, Schultz N, Thomas HD, et al. Specific killing of BRCA2-deficient tumours with inhibitors of poly(ADP-ribose) polymerase. Nature 2005;434:913–7.